ASM Sc. J., 12, Special Issue 1, 2019 for IQRAC2018, 117-125

Dual solutions in MHD Boundary Layer Flow of Carreau Fluid over a Shrinking Sheet with Convective Boundary Condition

Rusya Iryanti Yahaya[1], Norihan Md Arifin*[1,2], and Siti Suzilliana Putri Mohamed Isa[1]

[1] *Institute for Mathematical Research, Universiti Putra Malaysia, 43400 UPM Serdang Selangor, Malaysia*

[2] *Department of Mathematics, Universiti Putra Malaysia, 43400 UPM Serdang Selangor, Malaysia*

* *Corresponding author: norihana@upm.edu.my*

This paper studies on two-dimensional magnetohdrodynamics (MHD) boundary layer flow of Carreau fluid towards a non-linear shrinking sheet with convective boundary condition and non-linear thermal radiation. Appropriate similarity transformations are introduced to convert the governing equations into non-linear ordinary differential equations. The equations along with the transformed boundary conditions are then solved numerically using shooting method in Maple. The effects of various parameters such as the shrinking parameter, the suction parameter, the radiation parameter, the temperature ratio parameter, the magnetic parameter, the Prandtl number and the Biot number on the skin friction coefficient, the heat transfer rate, the fluid velocity and the fluid temperature are discussed and shown in tables and graphs. It is found that dual solutions are obtained at certain values of parameters and the higher the value of suction and magnetic parameter, the higher the heat transfer rate. As the radiation parameter increases, the fluid temperature decreases.

Keywords: Carreau fluid, MHD, shrinking sheet, suction, thermal radiation.

I. Introduction

There has been a growing interest in the study of fluid flow and heat transfer over a stretching/shrinking surface because of its wide applications in industry and engineering. According to Miklavčič and Wang (2006), the velocity of stretching sheet on the boundary is away from a fixed point while for shrinking sheet the velocity is towards a fixed point. The solution for stretching sheet would produce far field suction towards the sheet while shrinking sheet would produce velocity away from the sheet. Thus, the flow in shrinking sheet is unlikely to exist because the vorticity is not confined within a boundary layer. Miklavčič and Wang (2006) found that the flow can be maintained by having enough suction on the surface. Multiple solutions were found at certain suction rates. In a study by Fang (2008), it was found that the solutions may be non-unique or does not exist at larger shrinking rates. Later, in the study by Fang and Zhang (2010) and Bhattacharyya and Pop (2011) dual solutions were obtained at certain ranges of parameters.

Carreau fluid is a generalized Newtonian fluid that acts as power law fluid at high shear rate and as Newtonian fluid at low shear rate. Few studies have been carried out on Carreau fluid flow over shrinking surfaces. One of the studies was on stagnation point flow of MHD Carreau fluid which was done by Akbar et al. (2014). Hashim et al. (2017) extended this study by considering thermal radiation. Then, Hashim and Khan (2017) discussed the flow of MHD Carreau fluid past a shrinking cylinder where multiple solutions were found at certain ranges of parameters. Recently, the flow of Carreau fluid past an inclined shrinking surface was studied by Khan et al. (2018).

Due to the scarcity in the study of Carreau fluid flow over a shrinking sheet, this paper will study the flow of MHD Carreau fluid over a shrinking sheet. Suction and non-linear thermal radiation are considered in this problem. The governing equations are solved along the boundary conditions using shooting method in Maple. The results are then discussed in table and graphs.

II. Methodology

Consider a steady and incompressible two-dimensional boundary layer flow of Carreau fluid over a non-linear shrinking sheet with velocity $U_w = ax^m$, as shown in Fig. 1. Non-linear thermal radiation and convective boundary condition are taken into account in the heat transfer analysis. Cartesian coordinates are used to represents the problem such that the shrinking sheet is placed along the x-axis and y-axis is normal to it. The fluid is assumed to flow in the region $y \geq 0$. Magnetic field of strength B_0 is applied in the direction normal to the sheet and the induced magnetic field is not considered as the magnetic Reynolds number is assumed to be very small.

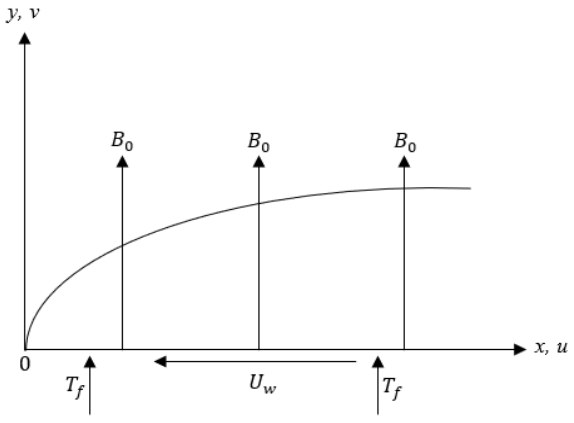

Figure 1: Physical model of the problem.

The governing equations for the stated problems are given as

$$\frac{\partial u}{\partial x} + \frac{\partial v}{\partial y} = 0, \tag{1}$$

$$u\frac{\partial u}{\partial x} + v\frac{\partial u}{\partial y} = \nu\frac{\partial^2 u}{\partial y^2}\left[1 + \Gamma^2\left(\frac{\partial u}{\partial y}\right)^2\right]^{\frac{n-1}{2}} + \nu(n-1)\Gamma^2\frac{\partial^2 u}{\partial y^2}\left(\frac{\partial u}{\partial y}\right)^2 \left[1 + \Gamma^2\left(\frac{\partial u}{\partial y}\right)^2\right]^{\frac{n-3}{2}} - \frac{\sigma B_0^2}{\rho}u, \tag{2}$$

$$u\frac{\partial T}{\partial x} + v\frac{\partial T}{\partial y} = \alpha\frac{\partial^2 T}{\partial y^2} - \frac{1}{\rho c_p}\frac{\partial q_r}{\partial y}, \tag{3}$$

subject to the boundary conditions

$$u = U_w(x) = ax^m, \quad v = v_w,$$
$$-k\frac{\partial T}{\partial y} = h_f(T_f - T) \quad \text{at} \quad y = 0, \tag{4}$$
$$u \to 0, \quad T \to T_\infty \qquad \text{as} \quad y \to \infty, \tag{5}$$

where u and v are the velocity components along the x and y directions respectively, ρ is the fluid density, $\nu = \frac{\mu}{\rho}$ is the kinematic viscosity of the fluid, Γ is the material constant called relaxation time, σ is the electrical conductivity of the fluid, n is the power law index, T is the fluid temperature, q_r is the radiative heat flux, $\alpha = \frac{k}{\rho c_p}$ is the thermal diffusivity with c_p represents the specific heat and k represents thermal conductivity of the fluid, $U_w(x)$ is the non-linear velocity with constants, $a < 0$ and $m > 0$ related to the shrinking speed, v_w is the mass transfer velocity, h_f is the convective heat transfer coefficient, T_f is the convective fluid temperature below the moving sheet and T_∞ is the ambient fluid temperature.

In the above equations, the power law index, n is used to determine the fluid behaviour. The value of $n = 1$ describes the fluid as Newtonian fluid. If the value of n is in the range of $0 < n < 1$, the behaviour of the fluid is of a shear-thinning fluid and when the value is $n > 1$, the fluid has the behaviour of a shear-thickening fluid.

Khan et al. (2016) stated that the radiative heat flux expression in Eq. (3) can be simplified using the Rosseland approximation,

$$q_r = -\frac{4\sigma^*}{3k^*}\frac{\partial T^4}{\partial y}, \tag{6}$$

where σ^* is the Stefan-Boltzmann constant and k^* is the mean absorption coefficient. In considering the flow over a horizontal flat plate, Eq. (6) can be written as follows

$$q_r = -\frac{16\sigma^*}{3k^*}T^3\frac{\partial T}{\partial y}. \tag{7}$$

By substituting Eq. (7) into Eq. (3), we obtain,

$$u\frac{\partial T}{\partial x} + v\frac{\partial T}{\partial y} = \frac{\partial}{\partial y}\left[\left(\alpha + \frac{16\sigma^* T^3}{3k^*\rho c_p}\right)\frac{\partial T}{\partial y}\right]. \tag{8}$$

Next, the following non-dimensional variables are introduced to simplify the mathematical analysis using similarity transformations,

$$\begin{aligned} \psi(x,y) &= \sqrt{\frac{2\nu b}{m+1}}x^{\frac{m+1}{2}}f(\eta), \\ \eta &= y\sqrt{\frac{b(m+1)}{2\nu}}x^{\frac{m-1}{2}}, \\ \theta(\eta) &= \frac{T-T_\infty}{T_f-T_\infty}, \end{aligned} \tag{9}$$

where η is the similarity variable with b as a constant and ψ is the stream function given by

$$u = \frac{\partial \psi}{\partial y} \quad \text{and} \quad v = -\frac{\partial \psi}{\partial x}. \tag{10}$$

From Eq. (9),

$$T = T_\infty[1 + (\theta_w - 1)\theta] \quad \text{with} \quad \theta_w = \frac{T_f}{T_\infty}, \tag{11}$$

where $\theta_w > 1$ is the temperature ratio parameter.

By substituting Eqs. (9)-(11) into Eqs. (1), (2), (4), (5) and (8), we obtain

$$\begin{aligned} &\left[1 + nWe^2(f'')^2\right]\left[1 + We^2(f'')^2\right]^{\frac{n-3}{2}} f''' \\ &+ ff'' - \left(\frac{2m}{m+1}\right)(f')^2 - M^2 f' = 0, \end{aligned} \tag{12}$$

$$\begin{aligned} &\theta'' + Prf\theta' \\ &\quad + \frac{4}{3N_R}\frac{d}{d\eta}[(1 + (\theta_w - 1)\theta)^3\theta'] = 0, \end{aligned} \tag{13}$$

$$f(0) = s, \quad f'(0) = \lambda, \quad \theta'(0) = -\gamma[1 - \theta(0)] \quad \text{at} \quad \eta = 0, \tag{14}$$

$$f'(\infty) \to 0, \quad \theta(\infty) \to 0 \quad \text{as} \quad \eta \to 0, \tag{15}$$

where the prime represents ordinary derivative with respect to η.

In the above equations, the local Weissenberg number, $We^2 = \frac{b^3(m+1)\Gamma^2 x^{3m-1}}{2\nu}$, the magnetic parameter, $M^2 = \frac{2\sigma B_0^2}{\rho b(m+1)x^{m-1}}$, the Prandtl number, $Pr = \frac{\mu c_p}{k}$, the non-linear radiation parameter, $N_R = \frac{kk^*}{4\sigma^* T_\infty^3}$, the local Biot number, $\gamma = \frac{h_f}{k}\sqrt{\frac{2\nu}{b(m+1)}}x^{\frac{1-m}{2}}$ and the shrinking parameter, $\lambda = \frac{a}{b}$ where $\lambda < 0$ for shrinking sheet. The mass transfer parameter is $s = -v_w\left(\sqrt{\frac{2}{\nu b(m+1)}}x^{\frac{1-m}{2}}\right)$ where $s > 0$ for suction and $s < 0$ for injection.

The local skin friction coefficient, C_{fx} and the local Nusselt number, Nu_x are given as follows

$$C_{fx} = \frac{\tau_w}{\rho U_w^2(x)}, \quad Nu_x = \frac{xq_w}{k(T_f - T_\infty)}, \tag{16}$$

where τ_w and q_w are the respective wall shear stress and wall heat transfer given by

$$\begin{aligned} \tau_w &= \mu\frac{\partial u}{\partial y}\left[1 + \Gamma^2\left(\frac{\partial u}{\partial y}\right)^2\right]^{\frac{n-1}{2}}\Bigg|_{y=0}, \\ q_w &= -k\left(\frac{\partial T}{\partial y}\right)_w + (q_r)_w. \end{aligned} \tag{17}$$

Equation (17) is substituted into Eq. (16) to obtain

$$\begin{aligned} Re^{1/2}C_{fx} &= \frac{1}{\lambda^2}\sqrt{\frac{m+1}{2}}f''(0) \\ &\quad [1 + We^2(f''(0))^2]^{\frac{n-1}{2}}, \\ Re^{-1/2}Nu_x &= -\sqrt{\frac{m+1}{2}}\theta'(0) \\ &\quad \left[1 + \frac{4}{3N_R}[1 + (\theta_w - 1)\theta(0)]^3\right], \end{aligned}$$

where $Re = \frac{bx^{m+1}}{\nu}$ is the local Reynolds number.

III. Results and Discussion

Differential equations (12) and (13) with the boundary conditions (14) and (15) are solved numerically using the shooting method in Maple. The equations and the method used are validated by comparing the present results of $f''(0)$ and local Nusselt number, $Re^{-1/2}Nu_x$ with other published results as shown in Table 1 and Table 2, respectively. The results are found to be in excellent agreement. Thus, it can be said that the equations and the method used in this study are accurate. In this problem, dual solutions are obtained at certain values of the parameters. Since we are only interested in studying the dual solutions of the problem, all the results shown in this paper are of two solutions. The stability analysis of dual solutions in Carreau fluid flow has been done by Naganthran and Nazar (2016) and Hashim et al. (2018). In these studies, the first solution is found to be stable while the second solution is unstable. Thus, the first solution is more realisable and physically meaningful than the second solution. It is expected that these findings hold in the present study. The behaviour of skin friction coefficient, $Re^{1/2}C_{fx}$ and local Nusselt number, $Re^{-1/2}Nu_x$ for various parameters involved in the flow equations are shown in table and graphs. The velocity profile and temperature profile for various parameters such as the shrinking parameter λ, suction parameter s, the radiation parameter N_R, the temperature ratio parameter θ_w, the magnetic parameter M, the Prandtl number Pr and the Biot number γ are also discussed.

The first solution and second solution of $Re^{1/2}C_{fx}$ and $Re^{-1/2}Nu_x$ for various values of M, s and λ are shown in Table 3. The first solution is chosen such that the solution is the first to approach the ambient fluid conditions asymptotically. In Table 3, the value of $Re^{1/2}C_{fx}$ of the first solution tends to increase when M increases while the opposite results are obtained for the second solution. The same behaviour is observed for $Re^{-1/2}Nu_x$.

The behaviour of $Re^{1/2}C_{fx}$ against various values of parameters are presented in Figs. 2-4. It can be seen from these figures that dual solutions exist when $\lambda > \lambda_c$, one solution at $\lambda = \lambda_c$ and no solution when $\lambda < \lambda_c$. The critical point, λ_c is the point at which the solutions are separated into two solutions. Figure 2 shows the variation of $Re^{1/2}C_{fx}$ with λ and M. As M increases, the value of $Re^{1/2}C_{fx}$ increases in the first solution and decreases in the second solution. This agrees with the results obtained in Table 3. In Fig. 3, the variation of $Re^{1/2}C_{fx}$ with λ and n is shown. It can be seen that the value of $Re^{1/2}C_{fx}$ for the first solution reduces as n increases while the opposite result is obtained for the second solution. Next, the variation of $Re^{1/2}C_{fx}$ with λ and s is illustrated in Fig. 4. The value of $|Re^{1/2}C_{fx}|$ increases in the first solution and decreases in the second solution as s increases.

The behavior of $Re^{-1/2}Nu_x$ against various values of parameters are illustrated in Figs. 5-7. In Fig. 5, the increase in M causes the value of $Re^{-1/2}Nu_x$ to increase in the first solution. This again agrees with the results obtained in Table 3. In Fig. 6, the value of $Re^{-1/2}Nu_x$ for the first solution decreases as n increases while the opposite result is observed for the second solution. The variation of $Re^{-1/2}Nu_x$ with λ and s can be observed in Fig. 7. The value of $Re^{-1/2}Nu_x$ in the first solution is noted to increase with s due to the increasing wall shear stress which increases the skin friction coefficient and then the heat transfer rate.

In Fig. 8, the increasing value of M causes the dimensionless fluid velocity profile, $f'(\eta)$ to increase in the first solution. In Fig. 9, the value of $f'(\eta)$ increases in the first solution and decreases in the other solution when the value of s increases. Besides that, the momentum boundary layer thickness for the first solution is observed to be smaller than the second solution. This is because, according to Zaimi and Ishak (2015), the increase in suction will increase the wall shear stress which then causes

the velocity gradient at the surface to increase.

The effect of M on the dimensionless temperature profile $\theta(\eta)$ is illustrated in Fig. 10. In general, the result for the first solution shows that the fluid temperature drops as M increases while the opposite behavior occurred in the other solution. Meanwhile, the effect of s on $\theta(\eta)$ is shown in Fig. 11 where the increase in suction causes the temperature to decrease in both of the solutions. Figure 12 shows that temperature profile decreases when N_R increases. Further, the effect of θ_w on temperature is presented in Fig. 13 where the increase in θ_w causes the fluid temperature profile to increase in both of the solutions. This is because when $\theta_w > 1$, the wall temperature is greater than the surrounding fluid temperature. This will cause the fluid temperature to arise. Furthermore, when γ is larger than 0.1, it indicates that heat convection occur between the shrinking sheet and the fluid. This can be seen by the results obtained in Fig. 14 which shows that the fluid temperature profile increases when the value of γ increases. Last but not least, it can be noted in Fig. 15 that the higher the value of Pr, the lower the temperature profile. This is because fluid with high Prandtl number has low thermal conductivity and thinner thermal boundary layer structures than fluid with low Prandtl number.

Table 1: Values of $f''(0)$ when $Pr = 1.5$, $We = 0.0$, $N_R = 1.0$, $T_w = 1.0$, $\gamma = 0.3$, $s = 1.0$, $M = \sqrt{2}$, $\lambda = -1$ and $n = 0.5$

m	$f''(0)$		
	Present	Ali et al. (2013)	Nadeem and Hussain (2009)
0.00	1.86201	1.86201	1.86201
0.25	1.76949	1.76949	1.76949
1.00	1.61803	1.61803	1.61804

IV. Conclusion

A steady, two-dimensional MHD flow of Carreau fluid over a non-linear shrinking sheet with convective boundary condition and non-

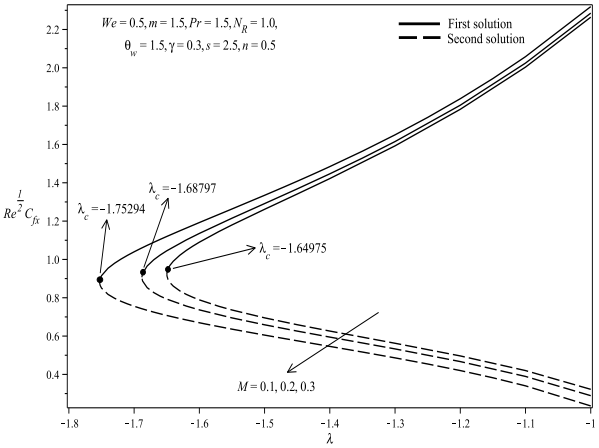

Figure 2: Variation of $Re^{1/2}C_{fx}$ with λ and M.

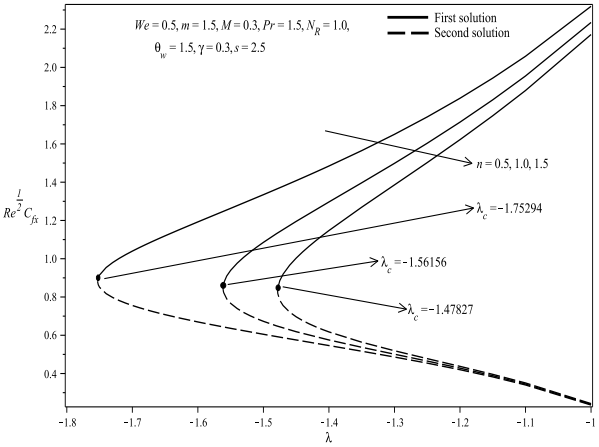

Figure 3: Variation of $Re^{1/2}C_{fx}$ with λ and n.

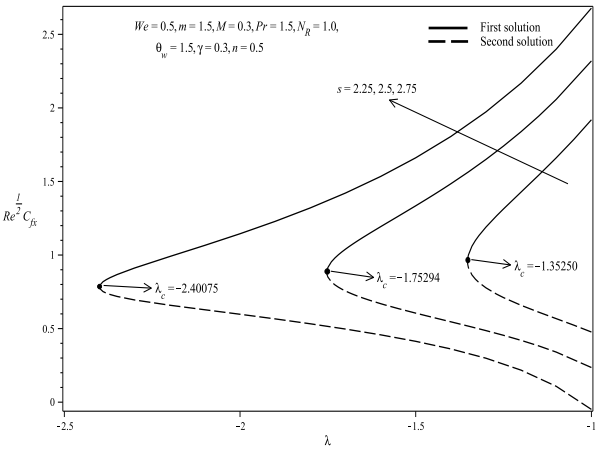

Figure 4: Variation of $Re^{1/2}C_{fx}$ with λ and s.

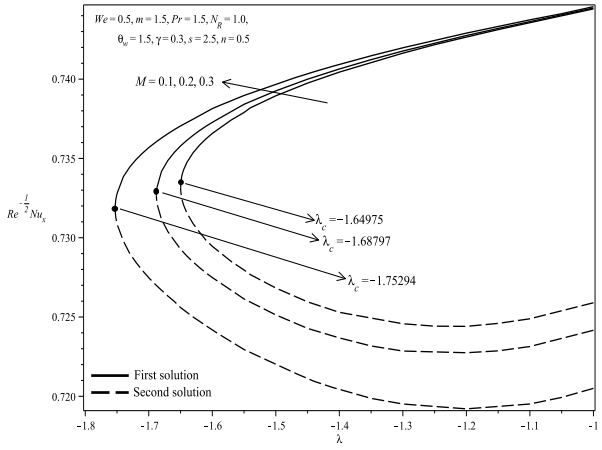

Figure 5: Variation of $Re^{-1/2}Nu_x$ with λ and M.

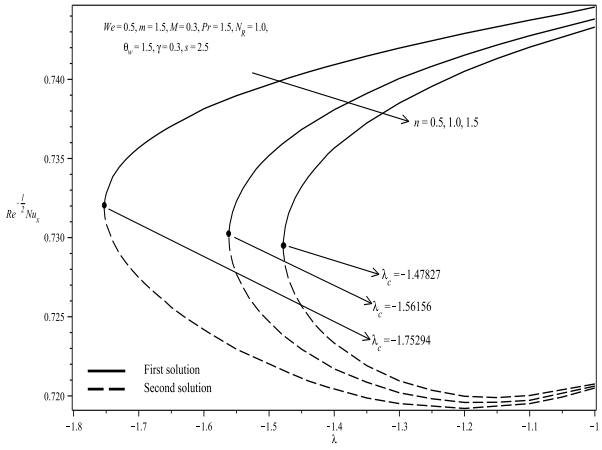

Figure 6: Variation of $Re^{-1/2}Nu_x$ with λ and n.

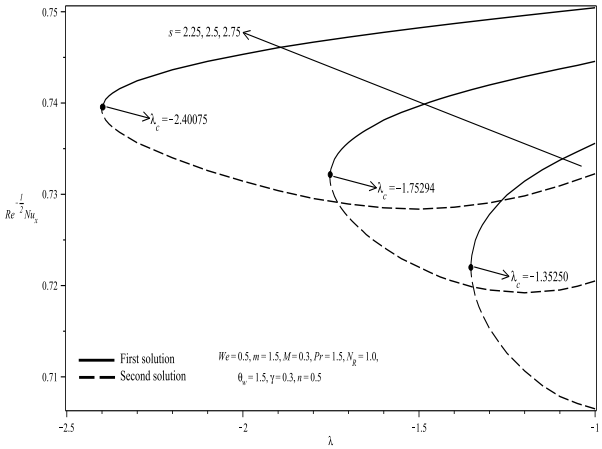

Figure 7: Variation of $Re^{-1/2}Nu_x$ with λ and s.

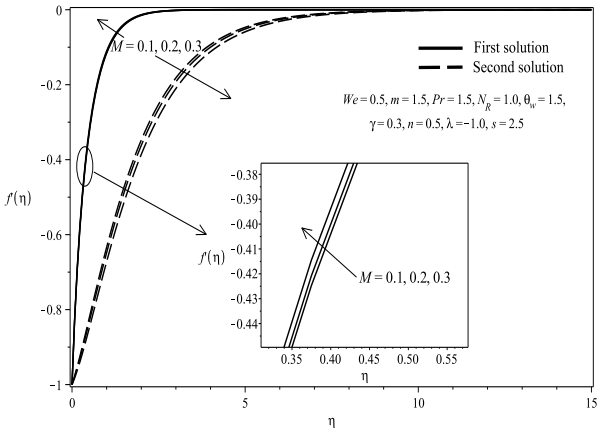

Figure 8: Effect of M on $f'(\eta)$.

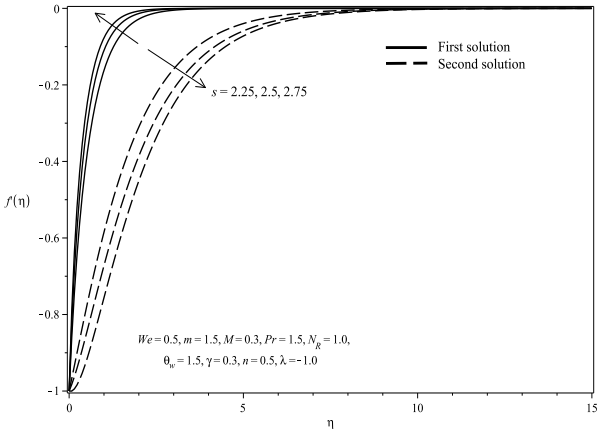

Figure 9: Effect of s on $f'(\eta)$.

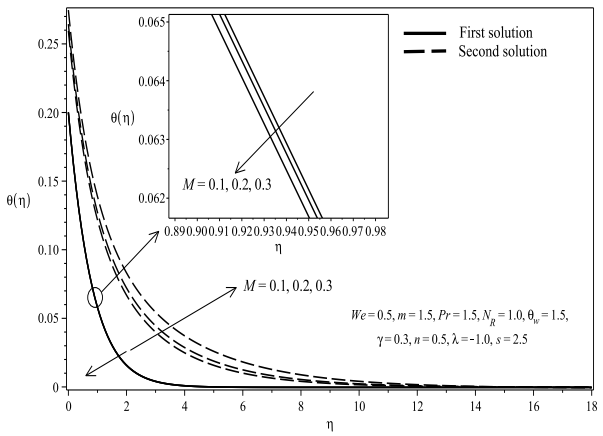

Figure 10: Effect of M on $\theta(\eta)$.

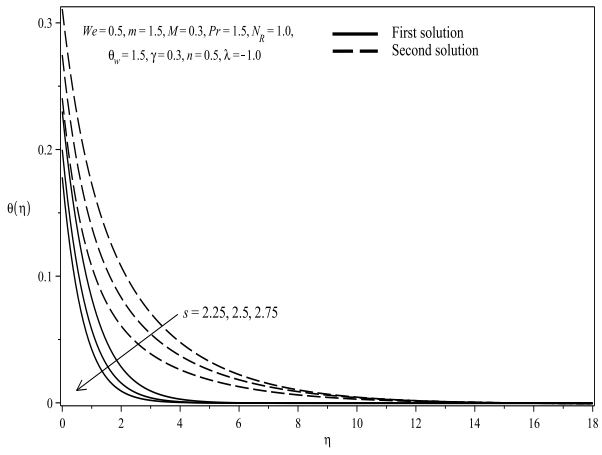

Figure 11: Effect of s on $\theta(\eta)$.

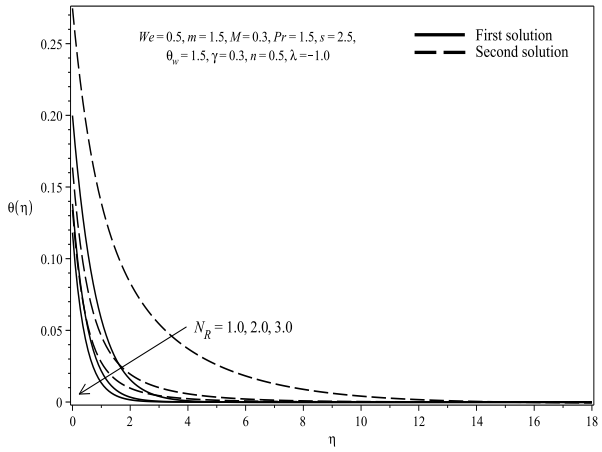

Figure 12: Effect of N_R on $\theta(\eta)$.

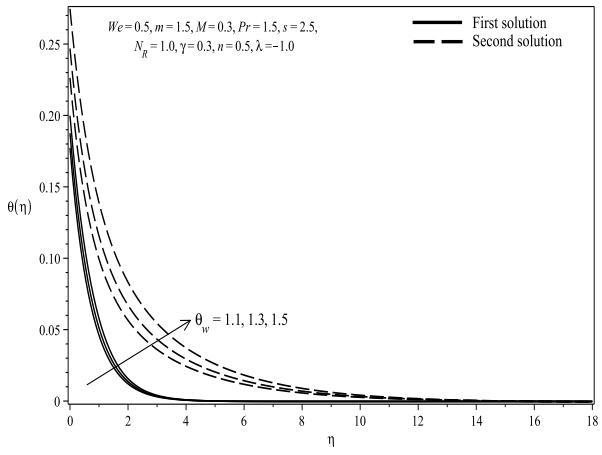

Figure 13: Effect of θ_w on $\theta(\eta)$.

Table 2: Values of $Re^{-1/2}Nu_x$ when $Pr = 1.5$, $We = 2.0$, $N_R = 1.0$, $T_w = 1.5$, $\gamma = 0.3$, $\lambda = 1.0$ and $m = 1.5$

s	M	$Re^{-1/2}Nu_x$			
		Present		Khan et al. (2016)	
		$n = 0.5$	$n = 1.5$	$n = 0.5$	$n = 1.5$
0.0	0.0	0.585085	0.613287	0.585077	0.613299
	0.5	0.565685	0.604028	0.565682	0.604028
	1.0	0.513371	0.579934	0.513053	0.579931

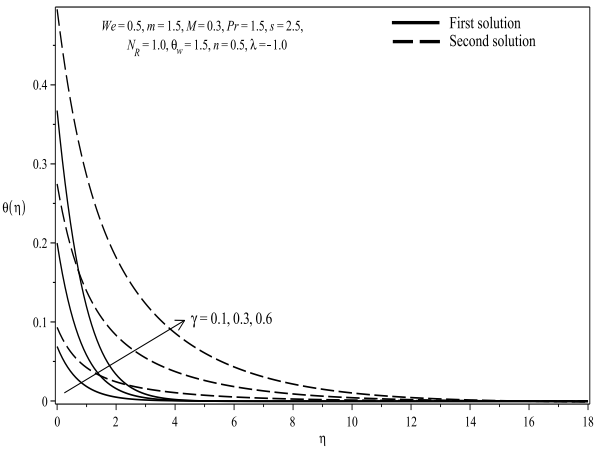

Figure 14: Effect of γ on $\theta(\eta)$.

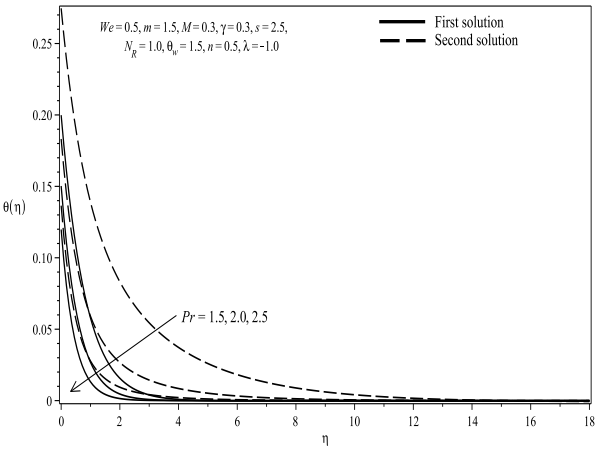

Figure 15: Effect of Pr on $\theta(\eta)$.

linear thermal radiation is studied. The governing equations and the boundary conditions are transformed using similarity transformations and then solved using shooting method. The effect of various parameters on the flow and thermal fields are discussed and shown in

Table 3: Values of $Re^{1/2}C_{fx}$ and $Re^{-1/2}Nu_x$ for various M, s and λ when $We = 0.5, Pr = 1.5, N_R = 1.0, \theta_w = 1.5, \gamma = 0.3$, $n = 0.5$ and $m = 1.5$

M	s	λ	$Re^{1/2}C_{fx}$		$Re^{-1/2}Nu_x$	
			First solution	Second solution	First solution	Second solution
0.1	2.50	-1.0	2.264106927	0.322118357	0.744427371	0.725897893
-	-	-1.3	1.592637751	0.562482462	0.741636791	0.724573939
-	-	-1.6	1.089932825	0.788926612	0.736574187	0.729458964
0.2	2.50	-1.0	2.285289766	0.289009753	0.744483679	0.724164111
-	-	-1.3	1.615126389	0.476845736	0.741772849	0.722853896
-	-	-1.6	1.135664725	0.736745912	0.737273604	0.727489710
0.3	2.25	-1.0	1.919315676	0.476845736	0.735587714	0.706494695
-	-	-1.3	1.190127002	0.776925855	0.727796062	0.715301859
-	2.50	-1.0	2.319334682	0.235297632	0.744568063	0.720501230
-	-	-1.3	1.650151260	0.486281010	0.741976504	0.719514253
-	-	-1.6	1.192490537	0.669590980	0.738140063	0.724187571
-	2.75	-1.0	2.678106048	-0.049254603	0.750437265	0.732248896
-	-	-1.3	1.973026608	0.298669092	0.749155560	0.729057014
-	-	-1.6	1.533875068	0.457725503	0.747742183	0.728518545

tables and graphs. The results can be summarized as follows:

1. Dual solutions exist when $\lambda > \lambda_c$.

2. The wall shear stress and heat transfer increase in the first solution, while decrease in the second solution when M and s increase.

3. The higher the value of M and s, the higher the value of $f'(\eta)$ in the first solution, while the opposite occurred in the other solution.

4. The increase in s and N_R cause the fluid temperature to decrease.

5. Large value of γ indicates that heat transfer occurred between the sheet and the surrounding fluid that causes the fluid temperature to increase.

6. Fluid with high value of Pr has low thermal conductivity and thin thermal boundary layer thickness.

Acknowledgements

The authors gratefully acknowledge the financial support received in the form of Putra Grant [9570600] from Universiti Putra Malaysia.

References

[1] N. S. Akbar, S. Nadeem, R. U. Haq, and S. Ye. MHD stagnation point flow of carreau fluid toward a permeable shrinking sheet: Dual solutions. *Ain Shams Engineering Journal*, 5(4):1233 – 1239, 2014.

[2] F. M. Ali, R. Nazar, N. M. Arifin, and I. Pop. Dual solutions in MHD flow on a nonlinear porous shrinking sheet in a viscous fluid. *Boundary Value Problems*, 2013(1):32, Feb 2013.

[3] K. Bhattacharyya and I. Pop. MHD boundary layer flow due to an exponentially shrinking sheet. 47:337–344, 12 2011.

[4] T. Fang. Boundary layer flow over a shrinking sheet with power-law velocity.

International Journal of Heat and Mass Transfer, 51(25):5838 – 5843, 2008.

[5] T. Fang and J. Zhang. Thermal boundary layers over a shrinking sheet: an analytical solution. *Acta Mechanica*, 209(3): 325–343, 2010.

[6] Hashim and M. Khan. Critical values in flow patterns of magneto-carreau fluid over a circular cylinder with diffusion species: Multiple solutions. *Journal of the Taiwan Institute of Chemical Engineers*, 77(Supplement C):282 – 292, 2017.

[7] Hashim, M. Khan, and A. S. Alshomrani. Numerical simulation for flow and heat transfer to carreau fluid with magnetic field effect: Dual nature study. *Journal of Magnetism and Magnetic Materials*, 443 (Supplement C):13 – 21, 2017.

[8] Hashim, M. Khan, A. S. Alshomrani, and R. U. Haq. Investigation of dual solutions in flow of a non-newtonian fluid with homogeneous-heterogeneous reactions: Critical points. *European Journal of Mechanics - B/Fluids*, 68:30 – 38, 2018.

[9] M. Khan, Hashim, M. Hussain, and M. Azam. Magnetohydrodynamic flow of carreau fluid over a convectively heated surface in the presence of non-linear radiation. *Journal of Magnetism and Magnetic Materials*, 412:63 – 68, 2016.

[10] M. Khan, H. Sardar, M. M. Gulzar, and A. S. Alshomrani. On multiple solutions of non-newtonian carreau fluid flow over an inclined shrinking sheet. *Results in Physics*, 8:926 – 932, 2018.

[11] M. Miklavčič and C. Y. Wang. Viscous flow due to a shrinking sheet. *Quarterly of Applied Mathematics*, 64(2):283–290, 2006.

[12] S. Nadeem and A. Hussain. MHD flow of a viscous fluid on a nonlinear porous shrinking sheet with homotopy analysis method. *Applied Mathematics and Mechanics*, 30(12):1569 – 1578, Dec 2009.

[13] K. Naganthran and R. Nazar. Stability analysis of MHD stagnation-point flow towards a permeable stretching/shrinking surface in a carreau fluid. *AIP Conference Proceedings*, 1750(1): 030031, 2016.

[14] K. Zaimi and A. Ishak. Boundary layer flow and heat transfer over a permeable stretching/shrinking sheet with a convective boundary condition. *Journal of Applied Fluid Mechanics*, 8(3):499–505, 2015.